

Physical realization and identification of topological excitations in quantum Heisenberg ferromagnet on lattice

Ranjan Chaudhury^a and Samir K. Paul^b

*S. N. Bose National Centre For Basic Sciences, Block-JD, Sector-III, Salt Lake
Calcutta-700098, India*

a) *ranjan021258@yahoo.com* , *ranjan@bose.res.in*

b) *smr@bose.res.in*

Physical spin configurations corresponding to topological excitations expected to be present in the XY limit of a purely quantum spin $\frac{1}{2}$ Heisenberg ferromagnet, are probed on a two dimensional square lattice . Quantum vortices (anti-vortices) are constructed in terms of coherent spin field components as limiting case of meronic (anti-meronic) configurations . The crucial role of the associated Wess-Zumino term is highlighted in our procedure . It is shown that this term can identify a large class of vortices (anti-vortices). In particular the excitations having odd topological charges form this class and also exhibit a self-similar pattern regarding the internal charge distribution .This manifestation of different behaviour of the odd and the even topological sectors is very prominent in the strongly quantum regime but fades away as we go to higher spins. Our formalism is distinctly different from the conventional approach for the construction of quantum vortices (anti-vortices).

PACS : 75.10. Jm ; 03.70. +k ; 03.75. Lm

Key Words : Topological, Ferromagnet, Wess Zumino, Vortices.

1. Introduction

The physical existence of topological excitations in quantum spin systems in one and two dimensions can be investigated by making use of various field theoretic techniques such as quantum action-angle representation, coherent state formulation and field theoretic approach manifesting a 'Berry Phase' [1-3]. The XY-limit of Heisenberg ferromagnet also belongs to this class of systems . It has been shown that in the case of a Heisenberg antiferromagnetic chain, the Wess-Zumino (WZ) term in the effective action is genuinely a topological term [1]. Moreover in the long wavelength limit of this system the explicit expression of this term is similar to that of the topological term for a nonlinear sigma model. Extending this approach further, it was shown by us [3] that it is possible to express the WZ term as a topological term, also in the case of a ferromagnetic chain in the long wavelength limit. Later we generalized this to the case of two dimensional ferromagnet [3,4] where again we demonstrated that in the above limit we could indeed get an expression from the WZ term , indicating the possibility of topological excitations.

Thus at this stage of analysis it is necessary to examine the physical configurations of these excitations in terms of coherent fields as well as the consequence of the WZ term, explicitly on a two dimensional square lattice. At the moment we do this for the XY-limit of the two dimensional Heisenberg ferromagnet with spin $\frac{1}{2}$. We show that the WZ term can indeed identify a large class of the topological excitations . Furthermore we demonstrate that this term can clearly differentiate between vortices (and antivortices) with different charges within this class. It is important to note that our entire analysis is valid for all temperatures .

2 Mathematical Formulation

2.1 Action and the Wess-Zumino term

The quantum Euclidean action \mathcal{S}_E for the spin coherent fields $\mathbf{n}(t)$, on a single lattice site , can be written as [2,3]

$$\mathcal{S}_E = -is\mathcal{S}_{WZ}[\mathbf{m}] + \int_0^\beta dt \mathcal{H}(\mathbf{n}) \quad (1)$$

where s is the magnitude of the spin ($s = \frac{1}{2}$ in the present case) and

$$\begin{aligned} \langle \mathbf{n} | \mathbf{S} | \mathbf{n} \rangle &= s\mathbf{n} \\ \mathcal{H}(\mathbf{n}) &= \langle \mathbf{n} | \mathcal{H}(\mathbf{S}) | \mathbf{n} \rangle \end{aligned} \quad (2)$$

$\mathcal{H}(\mathbf{S})$ being the single site effective spin Hamiltonian in spin (s) representation and $\mathcal{H}(\mathbf{n})$ is the corresponding Hamiltonian in the coherent spin fields, $\mathbf{n}(\mathbf{t})$. The variable t denotes the pseudo-time having the dimension of inverse temperature with $\beta = \frac{1}{kT}$ as usual, T being the real thermodynamic temperature of the spin system.

The Wess-Zumino term \mathcal{S}_{WZ} is given by (see Fradkin in Ref.[2])

$$\mathcal{S}_{WZ}[\mathbf{m}] = \int_0^\beta dt \int_0^1 d\tau \mathbf{m}(t, \tau) \cdot \partial_t \mathbf{m}(t, \tau) \wedge \partial_\tau \mathbf{m}(t, \tau) \quad (3)$$

with $\mathbf{m}(t, 0) \equiv \mathbf{n}(t)$, $\mathbf{m}(t, 1) \equiv \mathbf{n}_0$, and $\mathbf{m}(0, \tau) \equiv \mathbf{m}(\beta, \tau)$, $t \in [0, \beta]$, $\tau \in [0, 1]$.

The geometrical interpretation of equation(3) is that the left hand side represents the area of the cap bounded by the trajectory Γ , parametrized by $\mathbf{n}(t) [\equiv (n_1(t), n_2(t), n_3(t))]$ on the sphere:

$$\mathbf{n}(t) \cdot \mathbf{n}(t) = 1 \quad (4)$$

Furthermore the fields $\mathbf{m}(t, \tau)$ are the fields in the higher dimensional (t, τ) -space and the boundary values $\mathbf{n}(t)$ are the coherent spin fields. \mathbf{n}_0 is the fixed point $(0, 0, 1)$ on the sphere and the ket $|\mathbf{n}(t)\rangle$ appearing in the right hand side of equation (2), is the spin coherent state on a single lattice point [1-3]. For simplicity we have suppressed the coordinates in all the expressions.

For the whole two dimensional lattice, we express $\mathbf{n}(ia, ja, t)$ as $\mathbf{n}(ia, ja)$ for brevity, a being the lattice spacing. The WZ term for the whole lattice can formally be written as

$$\mathcal{S}_{WZ}^{tot} = \sum_{i,j=1}^{2N} \mathcal{S}_{WZ}[\mathbf{m}(ia, ja)] \quad (5)$$

However it is possible to evaluate only the 'difference' of $\mathcal{S}_{WZ}[\mathbf{m}(ia, ja)]$ terms at two neighbouring lattice sites in terms of the coherent spin fields $\mathbf{n}(ia, ja)$. Thus to extract the topological-like contribution from the total WZ term \mathcal{S}_{WZ}^{tot} , we use the following expressions for the above 'difference' (see Fradkin in Ref.[2]):

$$\begin{aligned} \delta_x \mathcal{S}_{WZ}[\mathbf{m}(\mathbf{r})] &= \mathcal{S}_{WZ}[\mathbf{m}(ia, ja)] - \mathcal{S}_{WZ}[\mathbf{m}((i-1)a, ja)] \\ &= \int_0^\beta dt [\delta_x \mathbf{n} \cdot (\mathbf{n} \wedge \partial_t \mathbf{n})](\mathbf{r}) \\ \delta_y \mathcal{S}_{WZ}[\mathbf{m}(\mathbf{r})] &= \mathcal{S}_{WZ}[\mathbf{m}(ia, ja)] - \mathcal{S}_{WZ}[\mathbf{m}(ia, (j-1)a)] \\ &= \int_0^\beta dt [\delta_y \mathbf{n} \cdot (\mathbf{n} \wedge \partial_t \mathbf{n})](\mathbf{r}) \end{aligned} \quad (6)$$

where

$$\begin{aligned} \delta_x \mathbf{n}(ia, ja) &= \mathbf{n}(ia, ja) - \mathbf{n}((i-1)a, ja) \\ \delta_y \mathbf{n}(ia, ja) &= \mathbf{n}(ia, ja) - \mathbf{n}(ia, (j-1)a) \end{aligned} \quad (7)$$

with $\mathbf{r} \equiv (ia, ja)$, and $i, j = 1, 2, \dots, 2N$.

We now write the following identity for the right hand side of equation (5):

$$\begin{aligned}
\mathcal{S}_{WZ}^{tot} &= \sum_{i,j=1}^{2N} \mathcal{S}_{WZ}[\mathbf{m}(ia, ja)] \\
&= \sum_{i,j=1}^{2N} \left[\frac{1}{2} \mathcal{S}_{WZ}[\mathbf{m}((i-1)a, ja)] + \frac{1}{2} \mathcal{S}_{WZ}[\mathbf{m}(ia, (j-1)a)] \right. \\
&\quad \left. + \frac{1}{2} \delta_x \mathcal{S}_{WZ}[\mathbf{m}(ia, ja)] + \frac{1}{2} \delta_y \mathcal{S}_{WZ}[\mathbf{m}(ia, ja)] \right] \quad (8)
\end{aligned}$$

The philosophy behind the above exercise was to extract the quantity which is directly calculable viz. difference in WZ term and cast it in the form analogous to that of the winding number in the case of a one dimensional system [2].

From equations (6), (7) and (8) we get

$$\begin{aligned}
2\mathcal{S}_{WZ}^{tot} &= \sum_{i,j=1}^{2N} \{ \mathcal{S}_{WZ}[\mathbf{m}((i-1)a, ja)] + \mathcal{S}_{WZ}[\mathbf{m}(ia, (j-1)a)] \\
&\quad - \int_0^\beta dt \mathbf{n}((i-1)a, ja) \cdot (\mathbf{n} \wedge \partial_t \mathbf{n})(ia, ja) \\
&\quad - \int_0^\beta dt \mathbf{n}(ia, (j-1)a) \cdot (\mathbf{n} \wedge \partial_t \mathbf{n})(ia, ja) \} \quad (9)
\end{aligned}$$

The pseudo-time derivatives of the coherent spin fields, $\partial_t \mathbf{n}(ia, ja)$ in the above equation can be expressed in terms of coherent fields at the above site and at the nearest neighbour sites through equations of motion which can be obtained from the action corresponding to the appropriate spin model on the lattice (see *Eqns.*(13), (14) and *Eqns.*(A.1), (A.2), (A.3) in the appendix). This brings out the topological character of the last two terms in the above expression of \mathcal{S}_{WZ}^{tot} . However the remaining terms (viz., 1st and the 2nd) in equation (9) have no such properties and hence we do not consider them for determination of topological charge. Therefore we keep only the topologically relevant terms and construct the following effective WZ -term :

$$\begin{aligned}
2\mathcal{S}_{WZ}^{effective} &= - \sum_{i,j=1}^{2N} \left\{ \int_0^\beta dt \mathbf{n}((i-1)a, ja) \cdot (\mathbf{n} \wedge \partial_t \mathbf{n})(ia, ja) \right. \\
&\quad \left. + \int_0^\beta dt \mathbf{n}(ia, (j-1)a) \cdot (\mathbf{n} \wedge \partial_t \mathbf{n})(ia, ja) \right\} \quad (10)
\end{aligned}$$

2.2 Action corresponding to spin model and equations of motion

The spin Hamiltonian corresponding to nearest neighbour anisotropic Heisenberg ferromagnet of XXZ type is given by[3]

$$\mathcal{H}(\mathbf{S}) = -g \sum_{\langle \mathbf{r}, \mathbf{r}' \rangle} \tilde{\mathbf{S}}(\mathbf{r}) \cdot \tilde{\mathbf{S}}(\mathbf{r}') - g\lambda_z \sum_{\langle \mathbf{r}, \mathbf{r}' \rangle} S_z(\mathbf{r}) S_z(\mathbf{r}') \quad (11)$$

with $g \geq 0$ and $0 \leq \lambda_z \leq 1$, \mathbf{r}, \mathbf{r}' running over the lattice, and $\langle \mathbf{r}, \mathbf{r}' \rangle$ signifies nearest neighbours with $\mathbf{S} \equiv (\tilde{\mathbf{S}}, S_z)$.

It follows from equations (2) and (11) that the total spin Hamiltonian on the lattice, in terms of coherent fields is given by

$$\mathcal{H}(\mathbf{n}) = -gs^2 \left[\sum_{\langle (i,j), (i',j') \rangle} \tilde{\mathbf{n}}(ia, ja) \cdot \tilde{\mathbf{n}}(i'a, j'a) + \lambda_z \sum_{\langle (i,j), (i',j') \rangle} n_z(ia, ja) n_z(i'a, j'a) \right] \quad (12)$$

Using equation (1) we can write the quantum action (Euclidean) for the two dimensional anisotropic ferromagnet as:

$$\begin{aligned} \mathcal{S}_E^{lattice} = & -is \sum_{i,j} \mathcal{S}_{WZ}[\mathbf{m}(ia, ja)] + \int_0^\beta dt [-gs^2 \sum_{\langle (i,j), (i',j') \rangle} \tilde{\mathbf{n}}(ia, ja) \cdot \tilde{\mathbf{n}}(i'a, j'a) \\ & -g\lambda_z s^2 \sum_{\langle (i,j), (i',j') \rangle} n_z(ia, ja) n_z(i'a, j'a)] \end{aligned} \quad (13)$$

where $s = \frac{1}{2}$, since we are considering the extreme quantum case.

The above action $\mathcal{S}_E^{lattice}$ is used to derive equations of motion as described in the previous section. We minimise $\mathcal{S}_E^{lattice}$ subject to the local constraint (4) on each lattice site. Thus we minimise the following quantity:

$$\mathcal{F}_{tot} = \mathcal{S}_E^{lattice} + \frac{1}{2} \int_0^\beta dt \sum_{(i,j)} a^2 \lambda_{i,j} [\mathbf{n}^2(i, j) - 1] \quad (14)$$

The 2nd term in the right hand side of the above equation is the lattice version of the term $\int d^2x \int_0^\beta \lambda(\mathbf{x}, t) (\mathbf{n}^2(\mathbf{x}, t) - 1)$ where $\lambda(\mathbf{x}, t)$ is an auxiliary field playing the role of a multiplier. The equations of motion which follow from the above minimisation are given in the Appendix A. We substitute the expressions for $\partial_t \mathbf{n}$ from Eqns. (A.1) into Eqn.(10). The purpose of this exercise is to obtain an approximate expression for $\mathcal{S}_{WZ}^{effective}$ given by equation (10) corresponding to the XXZ Heisenberg ferromagnet.

3. Calculations and Results

Now we present calculations for $\mathcal{S}_{WZ}^{effective}$ corresponding to vortices (anti-vortices) constructed out of coherent spin field components $n_1(ia, ja)$, $n_2(ia, ja)$ and $n_3(ia, ja)$. We analyse all the higher charged vortices by decomposing them in terms of elementary plaquettes of unit charge. We find that the odd-charged vortices can be described consistently by a flattened meron configuration. Even-charged vortices however, behave in an anomalous way.

3.1 Analysis of 1-vortex

Equation (10) shows that the summands are associated with the vertices 2, 3 and 4

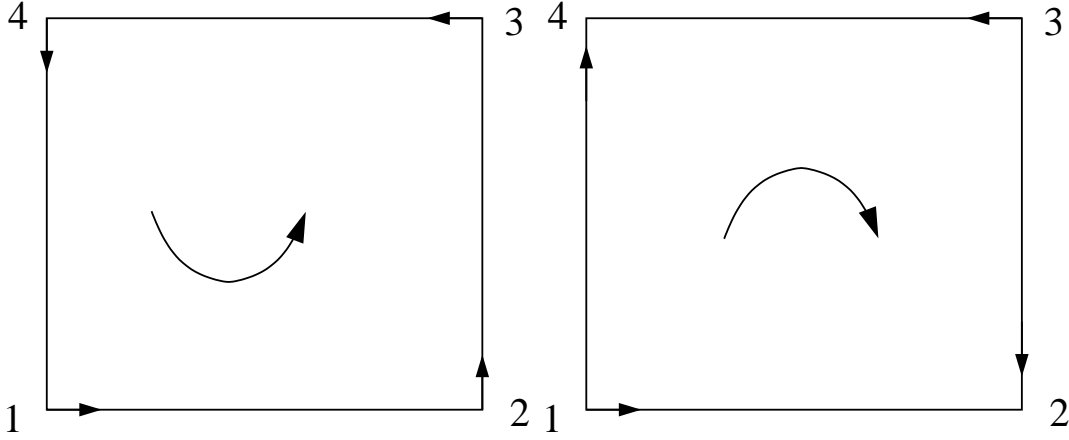


Fig. 1a

Fig. 1b

Figure 1: (a) 1-vortex , (b) 1-anti-vortex

where the vertices 1, 2, 3 and 4 of the 1-vortex [see Fig.1] are assigned the coordinates $(i-1)a, (j-1)a, (ia, (j-1)a), (ia, ja)$ and $((i-1)a, ja)$ respectively . The contribution of $\mathcal{S}_{WZ}^{effective}$ to a single plaquette [see Fig.1] with the above vertices can be written as (see Appendix) :

$$\begin{aligned}
[\mathcal{S}_{WZ}^{effective}]_{(1-vortex)} &= -\left\{ \int_0^\beta dt [\mathbf{n}((i-1)a, ja) \cdot (\mathbf{n} \wedge \partial_t \mathbf{n})(ia, ja) \right. \\
&\quad + \mathbf{n}(ia, (j-1)a) \cdot (\mathbf{n} \wedge \partial_t \mathbf{n})(ia, ja) \\
&\quad + \mathbf{n}((i-1)a, (j-1)a) \cdot (\mathbf{n} \wedge \partial_t \mathbf{n})(ia, (j-1)a) \\
&\quad \left. + \mathbf{n}((i-1)a, (j-1)a) \cdot (\mathbf{n} \wedge \partial_t \mathbf{n})((i-1)a, ja) \right\} \quad (15)
\end{aligned}$$

Now we focus our attention to the physical construction of vortices corresponding to our specific model . As we are interested in the extreme XY- anisotropic limit, we assume $n_3(i'a, j'a) = \sin \epsilon(i'a, j'a)$ at each lattice point $(i'a, j'a)$ where $\epsilon(i'a, j'a)$ is a very small positive quantity for each (i', j') . Then it follows from Eqn.(4) that within a vortex (or anti-vortex) the following conditions must be satisfied :

If one of the components n_1 (or n_2) at a vertex (la, ma) for $(l, m) = ((i-1), (j-1)), (i, (j-1)), (i, j)$ and $((i-1), j)$ is given by $\pm(1-\delta)$ then the other one is given by $\pm\sqrt{[\cos^2 \epsilon(la, ma) - (1-\delta)^2]}$; δ being small and positive , and assuming the same value at each vertex of the plaquette .

For illustration (see Fig.-1) we have a quantum vortex of charge +1 in which the horizontal arrow \rightarrow at a vertex represents n_1 with value $1-\delta$ and the vertical arrow \uparrow implies

n_2 with value $1 - \delta$. Further, in this figure the horizontal arrow \leftarrow at a vertex denotes n_1 having value $-(1 - \delta)$ and the vertical arrow \downarrow represents n_2 with value $-(1 - \delta)$. As shown in the appendix ; since the horizontal or vertical arrow has value $\pm(1 - \delta)$ for all time ,the quantity δ must be independent of time . It may be remarked that the vortex configuration (shown in Fig.1a) has a topological charge $+1$, as the spin rotates through an angle $+2\pi$ in traversing the boundary once in the anti-clockwise sense.

In this connection let us point out that usually in a two dimensional vortex corresponding to spin $\frac{1}{2}$ quantum spin model, the arrows \rightarrow and \uparrow signify eigenstates of S_x and S_y respectively having eigenvalues $+\frac{1}{2}$ [6]. The states \leftarrow and \downarrow are eigenstates of these operators respectively having eigenvalues $-\frac{1}{2}$. In our present formulation for quantum vortices, we make use of the spin coherent field components n_1 and n_2 to form vortex (anti-vortex), with $n_3(ia, ja) = \sin \epsilon(ia, ja)$ at each lattice point. Our picture is approximately that of flattened "meron(anti-meron) configurations" [7,8] mimicking a vortex (or anti-vortex) . This configuration arises naturally only when $\lambda_z \rightarrow 0$ *i.e.* in a pure XY model . As explained before, in this quantum vortex configuration n_1 or n_2 cannot be exactly equal to ± 1 . Rather we will have to choose them as $\pm(1 - \delta)$, where δ is an infinitesimal quantity. More detailed reasons are as follows:

If we want to identify the spin state $|\rightarrow\rangle$ (eigenstate of the operator S_x having eigenvalue $+\frac{1}{2}$) with the coherent state $|\mathbf{n}\rangle = \cos \frac{\theta}{2} |\frac{1}{2}\rangle + (e^{-\phi}) \sin \frac{\theta}{2} |-\frac{1}{2}\rangle$ corresponding to $s = \frac{1}{2}$, at a vertex [see Fig.1], we have $n_1 = 1, n_2 = 0$ and $n_3 = 0$ at that vertex. Similarly for $|\leftarrow\rangle$ we put $n_1 = -1, n_2 = 0$ and $n_3 = 0$; for $|\uparrow\rangle$ we have $n_1 = 0, n_2 = 1$ and $n_3 = 0$ and to represent $|\downarrow\rangle$ we require $n_1 = 0, n_2 = -1$ and $n_3 = 0$. In this way we can represent spin states at each vertex by the corresponding coherent spin states [see Eqn.(2)]. These assignments however violate the non-zero magnitude of n_3 , which is given by $n_3(la, ma) = \sin \epsilon(la, ma)$ at a vertex point of the vortex plaquette. Therefore we must choose n_1 or n_2 to be $\pm(1 - \delta)$ to preserve the constraint given by Eqn.(4) .

Let us now look at the symmetry properties of $\mathcal{S}_{WZ}^{effective}$. It can be shown that (see appendix) $\mathcal{S}_{WZ}^{effective}$ can easily be decomposed into two parts such that the first part changes sign in going over from a 1-vortex configuration to the corresponding anti-vortex configuration ; whereas the second part remains invariant under this operation. We denote the first part by B and the second part by A . This transformation from vortex to anti-vortex can be implemented by changing $n_2(2)$ and $n_2(4)$ in Fig.1 to $-n_2(2)$ and $-n_2(4)$ respectively. Algebraically this means that A contains terms which are of even degree in $n_2(2)$ and $n_2(4)$ whereas B contains terms that are linear or of odd degree in $n_2(2)$ and $n_2(4)$.

From Eqn.(15) we have $\mathcal{S}_{WZ}^{effective}$ in the form $A + B$ by using Eqn.(15) as explained in the Appendix A. :

3.2 Analysis of 2-vortex

For a typical 2-vortex we refer to Fig.2 . We calculate the contribution of $\mathcal{S}_{WZ}^{effective}$ given by equation (10) on such a plaquette by algebraically adding the contributions of $\mathcal{S}_{WZ}^{effective}$ on each of the individual elementary plaquettes (subvortices) with a weightage factor of $\frac{1}{2}$ to the common bonds shared between the pairs of adjacent subvortices. We denote these subvortices by a , b , c and d , each carrying topological charge $+1$ [Fig.2] . We are interested in those field configurations for which the contributions of $\mathcal{S}_{WZ}^{effective}$ on the common bonds cancel each other (see Appendix) and only the peripheral contribution on the boundary remains. However the spin at the central lattice point of the vortex (the point O in Fig.2) becomes ambiguous , as is clear from the fact that the spin configurations at the lattice points on the boundary of the plaquette cannot be shrunk to a unique spin at the centre . This is reflected through the fact that the horizontal effective spin at the centre vanishes. Thus the central point turns out to be a '**defect**' or a singular point. This brings peculiarities in the behaviour of the neighbouring spins as well , leading to the breakdown of the 2-vortex in the flattened meron configuration limit, if we construct the vortices in terms of elementary plaquettes . It can be explicitly demonstrated that this scenerio persists in the case of all other even-charged vortices as well (see Appendix)

Thus the contributions of $\mathcal{S}_{WZ}^{effective}$ on the boundary of the 2-vortex is not well defined . The scenerio persists in all the vortices (anti-vortices) possessing **even valued** topological charges , as can be read out from the spin field configuration in the case of 4-vortex [see Fig.4] .

3.3 Analysis of 3-vortex

For 3-vortex [see Fig. 3] however , we have a consistent spin field configuration . We have now an elementary anti-vortex plaquette at the central region with well defined field configurations , the contributions of $[\mathcal{S}_{WZ}^{effective}]$ along the common bond cancel giving rise to consistent spin field configurations . It may be pointed out that in contrast to the even-valued charge case we now have a subvortex with opposite charge occupying the central region. Studying the configuration in Fig. 3 , we discover the following identity

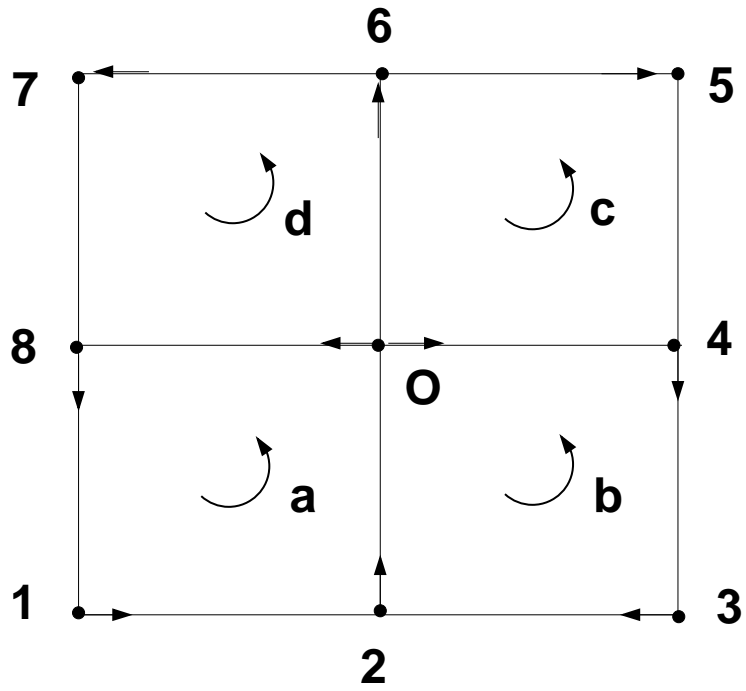


Figure 2: 2-vortex

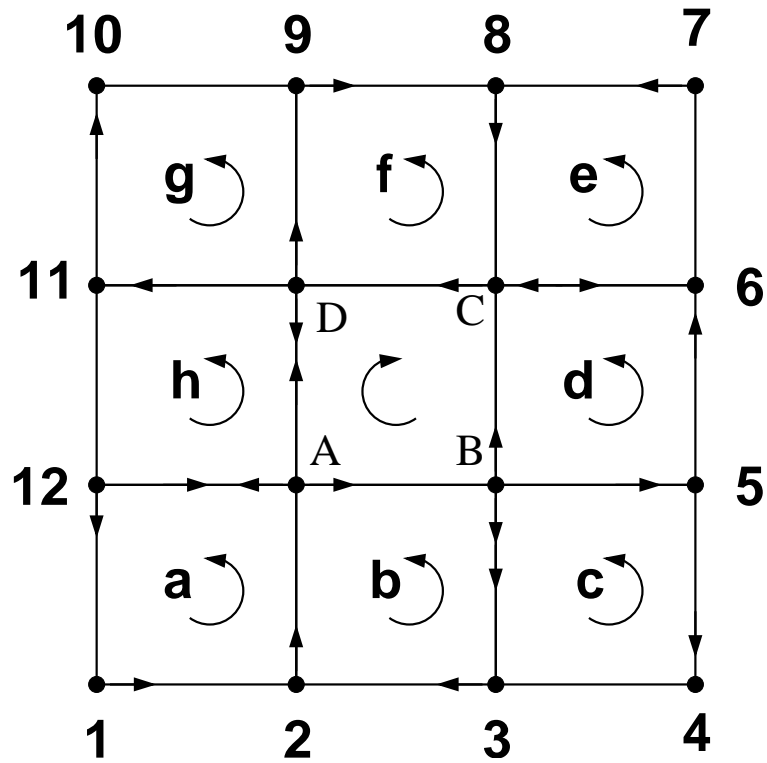


Figure 3: 3-vortex

for a topological Q -vortex, with odd values of Q ($Q \neq 1$), which describes the topological charge distribution inside the vortex consistently.

$$Q = \frac{1}{4}[Q^2 - (Q - 2)^2] + 1 \quad (16)$$

The quantity $(Q - 2)$ is the absolute value of the effective charge (negative) of the core which is an anti-vortex in this case. This can be generalized for Q -antivortex also. It may be pointed out that this equation is obtained directly by studying the charge distribution within these configurations. Notice that the above equation holds good even within the core, i.e., when Q is replaced by $(Q - 2)$, and thereby depicts a **self similar pattern**.

3.4 Analysis of 4-vortex

Here again [see *Fig. 4*] the spin at the centre becomes ambiguous, the horizontal effective

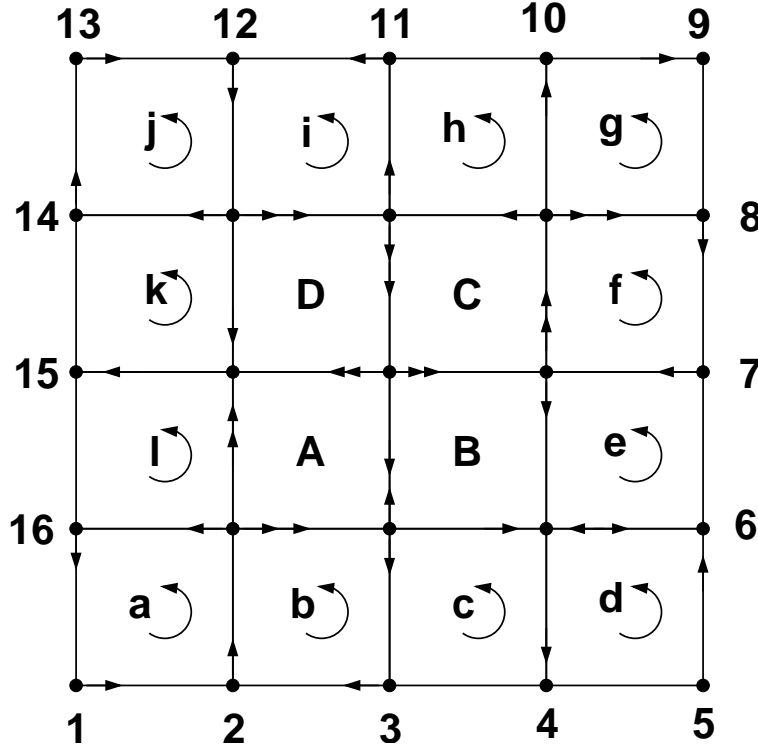


Figure 4: 4-vortex

spin at the centre vanishes. Once again the central point turns out to be a defect or a singular point, rendering cancellation of the contributions of $\mathcal{S}_{WZ}^{effective}$ on the common bonds impossible. The ambiguity of the suitable spin field configuration for 4-vortex is explained through equation () in the appendix.

4. Conclusion and Discussion

i) Our calculations and analysis with spin $\frac{1}{2}$ ferromagnetic quantum XY model in two

dimensions clearly bring out distinguishing features between even and odd charge sectors. The internal charge distribution equation [equation (30)] is obeyed by the excitations with odd charge in totality. The even charge sectors however are not governed by this equation.

ii) Our work has established the role of WZ term as a 'topological charge measuring quantity', obtained from microscopic theory. Furthermore, this term is able to test various internal consistencies and conservation conditions involving the topological charge distribution for a large class of excitations. Thus our approach is more powerful than that based on the heuristic operators suggested for determining the charges of topological excitations [6,9].

iii) Our future plan includes the generalization of our approach to the case of finite λ_z to achieve a physical realization of excitations of meronic type in the spin models. Furthermore, making use of these results and these configurations we aim to evaluate the static and dynamic spin correlations for spin $\frac{1}{2}$ anisotropic quantum Heisenberg ferromagnet at any temperature in two dimensions. These will contain contributions from both merons and anti-merons and are expected to exhibit distinguishing features from both even and odd topological charge sectors. These are of great importance in analysing the results from inelastic neutron scattering experiments, carrying the signature of the dynamics of these configurations themselves [7]. Our procedure can also throw some light on the possible phenomenological scenario of quantum Kosterlitz - Thouless transition [3,6,10].

iv) Last but not the least, the present investigation and methodology of ours may further be extended to low dimensional fermionic models[11] as well.

To conclude, this study of topological spin excitations on the 2D-lattice will undoubtedly play an important role in the understanding of thermodynamics of low dimensional ferromagnets.

Acknowledgement : One of the authors (SKP) would like to thank M.G.Mustafa, Rajarshi Roy and Purnendu Chakraborti for their valuable help in the preparation of the figures.

References

[1] Fradkin E and Stone M 1988 Phys. Rev. B 38 7215 ; Haldane F D M 1983 Phys. Rev.

- Letts. **50** 1153 ; Mikeska H J 1978 Jour. of. Phys. C **11** L29
- [2] Fradkin E 1991 Field Theories of Condensed Matter Systems (Addison-Wesley , CA) , Haldane F D M 1988 Phys. Rev. Letts. **61** 1029 ; Senthil T and Fisher M P A 2005 cond-mat/0510459
- [3] Chaudhury Ranjan and Paul Samir K 1999 Phys. Rev. B **60** 6234
- [4] Chaudhury Ranjan and Paul Samir K 2002 Mod. Phys. Letts. B **16** 251
- [5] Chaudhury Ranjan and Paul Samir K (To be communicated)
- [6] Loh E Jr., Scalapino D J and Grant P M 1985 Phys. Rev. B **31** 4712 ; Swendsen R H 1982 Phys. Rev. Lett. **49** 1302 ; Betts D D , Salevsky F C and Rogiers J 1981 J. Phys. A **14** 531
- [7] Berciu Mona and John Sajeev 2000 Phys. Rev. B **61** 16454 ; Mertens F G , Bishop A R, Wysin G M and Kawabata C 1987 Phys. Rev. Lett. **59** 117
- [8] Morinari T and Magn J 2006 Mag. Mat. **302** 382
- [9] Mól A S , Pereira A R , H. Chamati H and Romano S 2006 Eur. Phys. J. B **50** 541
- [10] Cuccoli A , Valerio T , Paola V and Ruggero V 1995 Phys. Rev. B **51** 12840 ; Kosterlitz J M and Thouless D J 1973 J. Phys. C **6** 1181 ; Berezinskii V L 1970 Sov. Phys. JETP **32** 493 , 1972 Sov. Phys. JETP **34** 610
- [11] Affleck Ian 1986 Nucl. Phys. B **265** [FS15] 409 ; Ribeiro T C , Seidel A , Han J H and Lee D H 2006 Europhys. Lett. **76(5)** 891

Appendix

Applying variational principle to the action given by equation (14), we obtain the equation of motion for an XY-anisotropic Heisenberg ferromagnet explicitly on the lattice , in the following form:

$$\begin{aligned}
\partial_t n_1(ia, ja) &= -i g s [\lambda_z n_2 N_3 - n_3 N_2](ia, ja) \\
\partial_t n_2(ia, ja) &= -i g s [n_3 N_1 - \lambda_z n_1 N_3](ia, ja) \\
\partial_t n_3(ia, ja) &= -i g s [n_1 N_2 - n_2 N_1](ia, ja)
\end{aligned} \tag{A.1}$$

In the above derivation we have used the following variation of the WZ-term given by (see Fradkin in Ref.[2])

$$\begin{aligned}
\delta \mathcal{S}_{WZ}^{tot}[\mathbf{m}] &= \sum_{i,j} \delta \mathcal{S}_{wz}[\mathbf{m}(ia, ja)] \\
&= \sum_{i,j} \int_0^\beta dt \delta \mathbf{n}(ia, ja) \cdot (\mathbf{n} \wedge \partial_t \mathbf{n})(ia, ja)
\end{aligned} \tag{A.2}$$

In Eqn.(A.1) $N_1(ia, ja)$, $N_2(ia, ja)$, $N_3(ia, ja)$ are the components of the vector \mathbf{N} at the lattice point (ia, ja) . The vector \mathbf{N} is given as:

$$\mathbf{N}(ia, ja) = \mathbf{n}(ia, (j-1)a) + \mathbf{n}((i-1)a, ja) + \mathbf{n}((i+1)a, ja) + \mathbf{n}(ia, (j+1)a) \quad (\text{A.3})$$

For the vortex (anti-vortex) plaquette having vertices 1 , 2 , 3 and 4 (see *Fig.1*) with coordinates $((i-1)a, (j-1)a)$, $(ia, (j-1)a)$, (ia, ja) and $((i-1)a, ja)$ respectively , it follows from Eqn.(10) that the contribution of $\mathcal{S}_{WZ}^{effective}$ to the 1-vortex is given by

$$\begin{aligned} [\mathcal{S}_{WZ}^{effective}]_{(1-vortex)} = & -\left\{ \int_0^\beta dt [\mathbf{n}((i-1)a, ja) \cdot (\mathbf{n} \wedge \partial_t \mathbf{n})(ia, ja) \right. \\ & + \mathbf{n}(ia, (j-1)a) \cdot (\mathbf{n} \wedge \partial_t \mathbf{n})(ia, ja) + \mathbf{n}((i-1)a, (j-1)a) \cdot (\mathbf{n} \wedge \partial_t \mathbf{n})(ia, (j-1)a) \\ & \left. + \mathbf{n}((i-1)a, (j-1)a) \cdot (\mathbf{n} \wedge \partial_t \mathbf{n})((i-1)a, ja) \right\} \end{aligned} \quad (\text{A.4})$$

We evaluate the right hand side of *Eqn.(A.4)* by substituting for $\partial_t \mathbf{n}$ from *Eqns.(A.1) and (A.3)* . To keep the calculations simple but consistent , we retain the intra-plaquette contributions by imposing a so called "local periodic boundary condition" (local PBC) as applied to the site closest to the vertices belonging to the plaquette under consideration .

In this case of 1-vortex [see *Fig.1a*] for the local PBC the field configurations satisfy

$$\begin{aligned} \mathbf{n}(ia, ja) &= \mathbf{n}((i-2)a, ja) = \mathbf{n}(ia, (j-2)a) \\ \mathbf{n}((i-1)a, ja) &= \mathbf{n}((i-1)a, (j-2)a) = \mathbf{n}((i+1)a, ja) \\ \mathbf{n}(ia, (j-1)a) &= \mathbf{n}(ia, (j+1)a) = \mathbf{n}((i-2)a, (j-1)a) \\ \mathbf{n}((i-1)a, (j-1)a) &= \mathbf{n}((i+1)a, (j-1)a) = \mathbf{n}((i-1)a, (j+1)a) \end{aligned} \quad (\text{A.5})$$

Besides we make use of the following conditions satisfied at different vertices of the plaquette for all time, as explained in the section 3.1 [see *Fig.1a*] :

$$\begin{aligned} n_1((i-1)a, (j-1)a) &= -n_1(ia, ja) = 1 - \delta \\ n_2(ia, (j-1)a) &= -n_2((i-1)a, ja) = 1 - \delta \end{aligned} \quad (\text{A.6})$$

This means that the following equations must hold :

$$\begin{aligned} \partial_t n_1((i-1)a, (j-1)a) &= -\partial_t n_1(ia, ja) = \partial_t(1 - \delta) \\ \partial_t n_2(ia, (j-1)a) &= -\partial_t n_2((i-1)a, ja) = \partial_t(1 - \delta) \end{aligned} \quad (\text{A.7})$$

Using Eqns. (A.1) , (A.4) and (A.5) we have

$$\partial_t n_1((i-1)a, (j-1)a) = -i g s \lambda_z n_2 N_3((i-1)a, (j-1)a)$$

$$\partial_t n_1(ia, ja) = -i g s \lambda_z n_2 N_3(ia, ja)$$

$$\partial_t n_2(ia, (j-1)a) = i g s \lambda_z n_1 N_3(ia, (j-1)a)$$

$$\partial_t n_2((i-1)a, ja) = i g s \lambda_z n_1 N_3((i-1)a, ja) \quad (\text{A.8})$$

The right hand sides of Eqns. (A.8) vanish in the flattened meron configuration limit where $\lambda_z \rightarrow 0$ and N_3 acquiring very small since $\epsilon(ia, ja)$ is very small in this configuration. Consequently from Eqns.(A.7) it follows that the quantity δ does not vary with time (δ is independent of the position of the vertex points of the plaquette [See Fig.1.a] , as explained in section 3.1)

Now using the Eqns. (A.1), (A.3), (A.5), (A.6) and (A.7) we obtain $\mathcal{S}_{WZ}^{effective}$ as follows :

$$\begin{aligned} [\mathcal{S}_{WZ}^{effective}]_{(1-vortex)} &= [n_1(2) + n_1(4)][(\mathbf{n} \cdot \mathbf{N})(3)n_1(3) - N_1(3)] \\ &+ [n_3(2) + n_3(4)][(\mathbf{n} \cdot \mathbf{N})(3)n_3(3) - N_3(3)] + n_1(1)[(\mathbf{n} \cdot \mathbf{N})(4)n_1(4) + (\mathbf{n} \cdot \mathbf{N})(2)n_1(2)] \\ &+ n_2(1)[(\mathbf{n} \cdot \mathbf{N})(4)n_2(4) + (\mathbf{n} \cdot \mathbf{N})(2)n_2(2) - 2N_2(2)] + n_3(1)[(\mathbf{n} \cdot \mathbf{N})(4)n_3(4) \\ &+ (\mathbf{n} \cdot \mathbf{N})(2)n_3(2) - 2N_3(2)] \\ &= A + B \end{aligned} \quad (\text{A.9})$$

where A and B are given by:

$$\begin{aligned} A &= \int_0^\beta dt \{2(n_1(2) + n_1(4))^2[n_1^2(3) - 1] + 2 n_1(3) n_3(3) [n_1(2) + n_1(4)][n_3(2) + n_3(4)] \\ &+ 4 n_2(1) [n_2^2(2) - 1][n_2(3) + n_2(1)]\} \\ B &= \int_0^\beta dt \{+2 n_2(2) n_1(1) [n_1(2) - n_1(4)] [n_2(3) + n_2(1)] \\ &+ 2 n_2(2) n_3(1) [n_3(2) - n_3(4)] [n_2(3) + n_2(1)]\} \end{aligned} \quad (\text{A.10})$$

It is interesting to note that A remains invariant if we go from vortex to antivortex by changing $n_2(2)$ and $n_2(4)$ in *Fig.1* to $-n_2(2)$ and $-n_2(4)$ respectively whereas B goes over to $-B$. Thus $[\mathcal{S}_{WZ}^{effective}]_{(1-vortex)}$ takes the form $A - B$ for antivortex [*Fig1.b*].

To analyse the case of 2- vortex [*Fig.2*] we assign the co-ordinates to the vertices 1, 2, 3, 4, 5, 6, 7, 8 as $((i-1)a, (j-1)a)$, $(ia, (j-1)a)$, $((i+1)a, (j-1)a)$, $((i+1)a, ja)$, $((i+1)a, (j+1)a)$, $(ia, (j+1)a)$, $((i-1)a, (j+1)a)$, $((i-1)a, ja)$ respectively. The centre O has co-ordinates (ia, ja) . Using Eqns. (A.1), (A.3) as well as the local PBC; the equations motion of the spins n_2 at the vertices 2, 4, 6, 8 reduce to the following, in the flattened meron configuration limit ($\lambda_z \rightarrow 0$):

$$(1 - \delta)^2 = \cos^2\epsilon(2) = \cos^2\epsilon(4) = \cos^2\epsilon(6) = \cos^2\epsilon(8) \quad (\text{A.11})$$

It is therefore obvious from the above equations that the z-component of the spin \mathbf{n} viz., n_3 becomes position independent.

In *Fig.3* we have denoted the elementary vortex plaquettes by **a, b, c, d, e, f, g, h**. Note that there is an elementary anti-vortex plaquette in the central region with vertices **A, B, C** and **D**. We write formally the expression for $[\mathcal{S}_{WZ}^{effective}]_{(3-vortex)}$:

$$\begin{aligned} & [\mathcal{S}_{WZ}^{effective}]_{(3-vortex)} = \\ & \int_0^\beta dt \{ \mathbf{n}(1a) \cdot (\mathbf{n} \wedge \partial_t \mathbf{n})(2a) + \frac{1}{2} \mathbf{n}(2a) \cdot (\mathbf{n} \wedge \partial_t \mathbf{n})(3a) + \frac{1}{2} \mathbf{n}(4a) \cdot (\mathbf{n} \wedge \partial_t \mathbf{n})(3a) + \mathbf{n}(1a) \cdot (\mathbf{n} \wedge \partial_t \mathbf{n})(4a) \\ & + \mathbf{n}(1b) \cdot (\mathbf{n} \wedge \partial_t \mathbf{n})(2b) + \mathbf{n}(2b) \cdot (\mathbf{n} \wedge \partial_t \mathbf{n})(3b) + \frac{1}{2} \mathbf{n}(4b) \cdot (\mathbf{n} \wedge \partial_t \mathbf{n})(3b) + \frac{1}{2} \mathbf{n}(1b) \cdot (\mathbf{n} \wedge \partial_t \mathbf{n})(4b) \\ & + \frac{1}{2} \mathbf{n}(1c) \cdot (\mathbf{n} \wedge \partial_t \mathbf{n})(2c) + \mathbf{n}(2c) \cdot (\mathbf{n} \wedge \partial_t \mathbf{n})(3c) + \mathbf{n}(4c) \cdot (\mathbf{n} \wedge \partial_t \mathbf{n})(3c) + \frac{1}{2} \mathbf{n}(1c) \cdot (\mathbf{n} \wedge \partial_t \mathbf{n})(4c) \\ & + \dots \\ & + \frac{1}{2} \mathbf{n}(1h) \cdot (\mathbf{n} \wedge \partial_t \mathbf{n})(2h) + \frac{1}{2} \mathbf{n}(2h) \cdot (\mathbf{n} \wedge \partial_t \mathbf{n})(3h) + \frac{1}{2} \mathbf{n}(4h) \cdot (\mathbf{n} \wedge \partial_t \mathbf{n})(3h) + \mathbf{n}(1h) \cdot (\mathbf{n} \wedge \partial_t \mathbf{n})(4h) \} \end{aligned} \quad (\text{A.12})$$

In the above equation (1a), (2a), (3a) and (4a) denote the vertices for the subvortex **a** in the anti-clockwise sense as we have already used in the case of 1-vortex. Similarly for the other subvortices. It can be shown after a long calculation that Eqn. (A.13) can be written in the form $A + B$, as we had in the case of 1-vortex, where B consists of terms linear in $n_2(2)$ or containing odd powers of $n_2(2)$. Thus $A + B$ over goes to $A - B$ as we

go from vortex to anti-vortex.

In the case of a 4-vortex [Fig.4] we have again a single lattice point as in the case of the 2-vortex. By similar reasons the 4-vortex construction in terms of elementary plaquettes, breaks down in the flattened meron configuration limit.